Aquamarine from Massangana batholith, Rondônia State: mineral chemistry and fluid inclusion data

Ingrid de Souza Hoyer[1,3]
  https://orcid.org/0000-0001-7278-4375
Valmir da Silva Souza[1,4]
  https://orcid.org/0000-0002-4957-5951
Beatriz Pereira Debowski[2,5]
  https://orcid.org/0000-0002-4935-0832

[1]Universidade de Brasília - UnB, Instituto de Geociências, Brasília - Distrito Federal - Brasil.

[2]Universidade Estadual do Rio de Janeiro – UERJ, Faculdade de Geologia, Rio de Janeiro - Rio de Janeiro - Brasil.

E-mails: [3]ingridshoyer@gmail.com, [4]valmirsouzaunb@gmail.com, [5]biadebowski@gmail.com

Abstract

Beryl is usually found in granite-pegmatite systems. The addition of chromophore elements (V, Cr, Mn, Fe) into the crystalline structure favors color changes in beryl and thus generates some of the world's expensive gems such as emerald, morganite, heliodor and aquamarine. The Massangana polyphasic batholith is a well-known cassiterite, wolframite and gems deposit in the Rondônia state. These metals and blue-gems (topaz and aquamarine) are located in feldspar-rich pegmatite granite bodies. The aquamarine crystals show color ranging from light- to medium-blue and display concentric growth zones. Electron-probe microanalyses revealed that the Fe is the main chromophore element, occupying the octahedral Al-site, while Na had an important role in the charge balance, inserted in the channel sites together with H_2O. The irregular supply of Fe and Na during the nucleation and growth of aquamarine was the main cause for the color change. A fluid inclusion study indicated that the aquamarine growth under an aqueous fluid system (H_2O-NaCl), with low salinity, low density and total homogenization temperature between 243º-315º C, is compatible with final temperatures in the pegmatite pocket zone.

Keywords: aquamarine, Massangana batholith, Rondônia, electron probe microanalysis (EPMA), mineral chemistry, microthermometry, fluid inclusion.

1. Introduction

Gem-quality beryl is usually found in fractionated-granitic or granite-pegmatite systems. Beryl is a cyclosilicate with its simplest chemical formula $Be_3Al_2[Si_6O_{18}]$, organized in hexagonal rings of Si-tetrahedra structure parallel to (0001), cross-linked together both by Be-tetrahedra and Al-octahedra sites, forming a three-dimensional framework. This crystalline structure has channels parallel to the c-axis that may host alkali, H_2O and CO_2 molecules, favoring complex replacement by other cations, such as Fe^{2+}, Mn^{2+}, Mg^{2+} and Li^+ (Morosin, 1972; Aurisicchio *et al.*, 1988; Sherriff *et al.*, 1991; Artioli *et al.* 1993). The addition of the chromophore elements (Cr, V, Mn, Fe) into the Al-structure favors color changes in beryl (Hawthorne and Huminicki, 2002), and thus generating some of the world's expensive gems such as emerald (Cr, V), morganite (Mn), heliodor (Fe, Mn) and aquamarine (Fe).

Brazil is a world's producer of aquamarine, whose main deposits are in Minas Gerais, Espírito Santo, Bahia, Paraíba, Rio Grande do Norte and Rondônia states (CPRM 2007, Barreto and Bittar 2010). In the Rondônia state, the Massangana batholith is a well-known cassiterite and wolframite deposit, as well as producer of some gems (mainly topaz and beryl), which have been exploited applying an artisanal mining-type known as "garimpo". In this deposit, the metals and gems occurs within pegmatites and hydrothermal veins, but also occur in paleo-alluvial deposits. Despite these gems being known and traded over time, information about the gemological quality and mineralogical properties are still insufficient or inexistent (e.g. Souza *et al.*, 2003; Debowski *et al.*, 2013). Herein, we report on chemistry and fluid inclusion compositions of aquamarine, a blue variety of beryl from Massangana batholith, thus adding information about the mineralogical characteristics and the physical-chemical nature of the paleofluids trapped in this gem.

2. Analytical methods

All analytical procedures were performed at the laboratories at the Geoscience Institute of the Brasília University (IG-UnB). The studied samples were cut in tablets, with orientations parallel and perpendicular (basal section) to the c-axis. A thin section cut was made according to the basal plane of the sample for petrographic and electron probe microanalysis (EPMA). In addition, two double-polished thin sections (around 1 mm thickness), cut according to the basal plane and to the c-axis, were prepared for the study of fluid inclusions.

The chemical composition of aquamarine was obtained through electron probe microanalysis techniques (EPMA). A JEOL JXA-8230 microanalyzer with five coupled wavelength dispersive spectrometers (WDS) was used. The analytical conditions applied were: accelerating voltage of 20 kV, beam current of 40 nA, beam diameter of 1–2 μm, and counting times of 15 and 10 s for peak and background positions, respectively. The data reduction was performed with the ZAF program and the following standards were used: microcline (K, Al, Si), albite (Na), andradite (Ca, Fe), forsterite (Mg), pyrophanite (Mn, Ti), chromite (Cr) and pollucite (Cs). The results are reported as wt.% oxide, and the number of ions in mineral formula were calculated on the basis of 3 Be and 18 O atoms per formula unit (apfu). For H_2O content calculation, the equation proposed by Marshall *et al.*, (2016) was applied.

The microthermometric measurements were carried out using a LINKAM THMS-600 heating-freezing system coupled to an Olympus BX-51 petrographic microscope with 10x and 50x long distance objectives. The calibration-stage was performed using synthetic fluid inclusion standards, applying speed rates from 10º to 5º C/min, with an estimated accuracy of ± 0.3º C for the freezing (+25º to -100ºC) and ± 5º C for the heating (up to 400ºC).

3. Geological setting

In the State of Rondônia occurs several Meso- to Neoproterozoic rapakivi granitic associations (Fig. 1a), emplaced during successive magmatic episodes between 1606 and 974 Ma, which make up the so-called Rondônia Tin Province (Kloosterman, 1968; Priem *et al*, 1966 and 1971; Leal *et al.*, 1978; Isotta *et al.*, 1978; Bettencourt *et al.*, 1999; CPRM, 2007). However, the most significant metal concentrations (Sn, W, Nb, Ta) and gems are associated to A-type highly-fractionated magmatic episodes, occurred between 1314 and 974 Ma, and are represented by São Lourenço-Caripunas (1314-1309 Ma), Santa Clara (1082-1074 Ma) and Rondônia (995-974 Ma) intrusive suites (Bettencourt *et al.*, 1999).

The Massangana batholith belongs to the Rondônia Suite, and intrudes the Paleoproterozoic basement rocks of the Jamari Complex (Isotta *et al.*, 1978; CPRM, 2007). It is a polyphasic granitic system with outstanding contrast through remote sensor and aerogeophysical products, marked by its ESE-WNW elliptical shape with ring-fault structure (Fig. 1b), and related to the successive magmatic phases (Kloosterman, 1967; Priem *et al.*, 1971; Okida, 2001; CPRM, 2007). Four alkaline magmatic phases have been recognized (Fig. 1b): Massangana, Bom Jardim, São Domingos and Taboca, which are close in age (1096 – 993 Ma). The Massangana is the main and oldest phase composed of coarse rapakivi biotite-alkali-fedspar granite. The Bom Jardim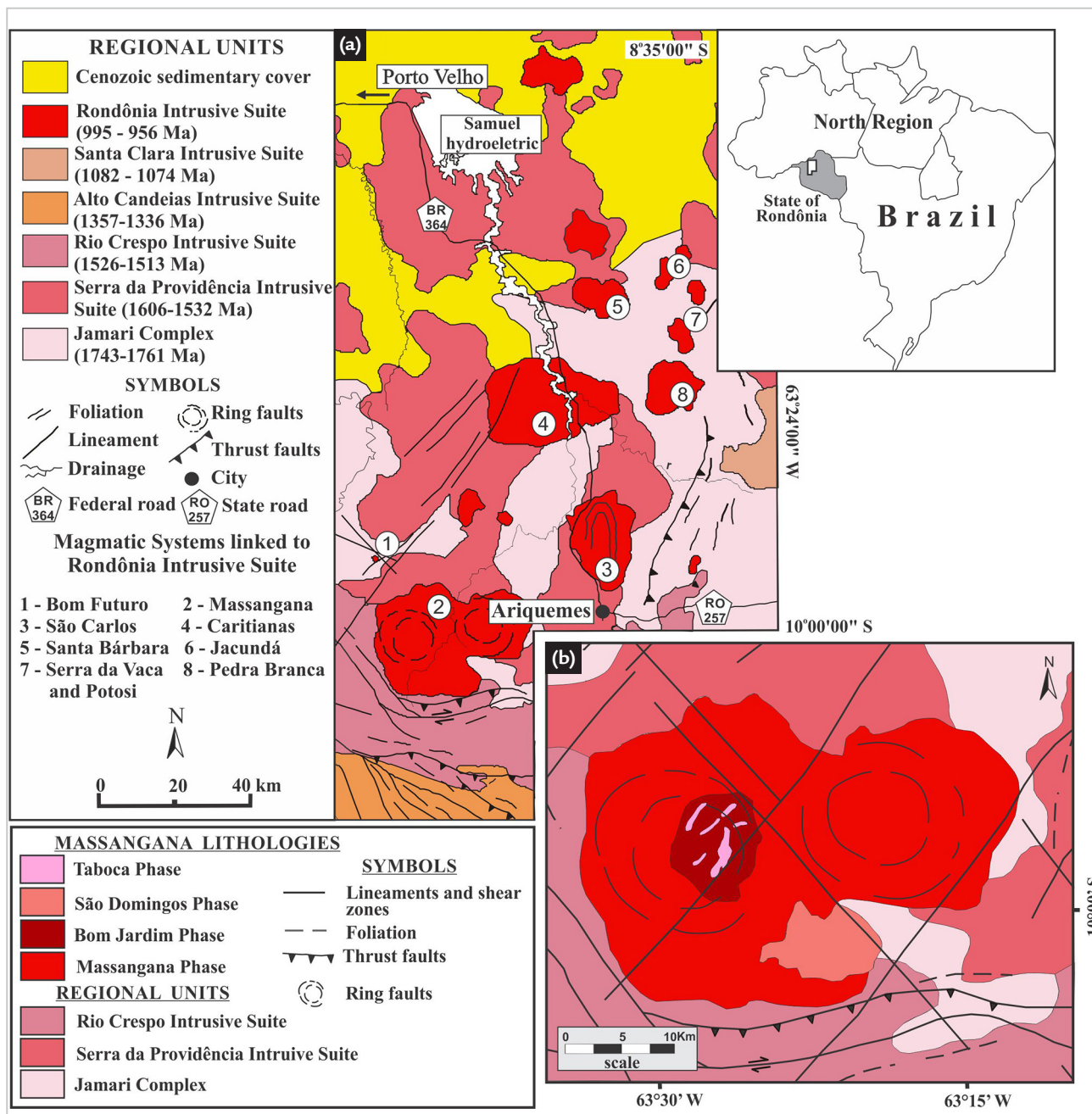 and São Domingos phases are intrusive in the Massangana phase and composed of inequigranular biotite granites. Taboca is the youngest phase. It is composed of inequigranular syenite to quartz-syenite apophyses and intrudes the Bom Jardim phase (Priem *et al.*, 1966; Romanini, 1982; Bettencourt *et al.*, 1999; CPRM, 2007; Debowski, 2016).

Blue-gems, topaz and aquamarine, are located in feldspar-rich pegmatite granite bodies, related to the Bom Jardim and São Domingos phases. The pegmatites are often found within the contact zone between granite and Jamari Complex wall rocks, but may also occur in the granite. They are morphologically tabular to irregular shape, texturally simple or asymmetrically zoned, show medium to coarse grained, and their thickness and continuity are variable

(Fig. 2a). Generally, these pegmatites present the following zonal sequence: a cortex of elongated biotite crystals radially arranged or in comb texture, marking the wall- or border-zone. The intermediate zone is dominant and composed of K-feldspar (partially altered to kaolin) quartz, mica (biotite) and Na-plagioclase (also argilized) inequigranular aggregates, whose crystals reach a size up to 1.5 cm. In this zone, there also occur disseminated crystals of fluorite, topaz, cassiterite, wolframite, columbite-tantalite and some sulfides. In the core-or pocket-zone, which is lenticular, the blue-gems (topaz and aquamarine) occur normally associated with quartz, cassiterite, wolframite columbite-tantalite and fluorite. In this place, the mineral assemblage may reach sizes above 5 cm, normally embedded in kaolin.

Figure 1 - a) Geological map of the central-northern portion of State of Rondônia, highlighting the granitic systems that make up the Rondônia Tin Province (modified from CPRM, 2007); b) Geological map of the Massagana polyphasic batholith (Debowski, 2016).

4. Chemistry data

The aquamarine is represented by euhedral to subhedral short to long crystals (Fig. 2b), slight to moderate fractured, with concentric growth zones and color ranging from light- to medium-blue. Frequently, the growth zones host some micro-inclusions (mainly feldspars and mica), but opaque and clay minerals also occur (Fig. 2c).

Representative EPMA analyses for 30 different spots are summarized in Table 1. However, in Figure 2c, only part of these analyses are indicated (15 in total), which can be used to illustrate and verify the chemical variations inside the aquamarine crystal. The stoichiometric calculation results identified in Table 1 are applied due to the difficulty in obtaining EPMA accurate analytical results for Be and H_2O (Groat *et al.*, 2002). Therefore, the sum of the oxides goes to below 100 wt.% (commonly between 97 and 99 wt.%).

Table 1 - Intervals of EPMA analysis of the 30 different spots obtained in aquamarine crystal. The number of ions in mineral formula were calculated on the basis of 3 Be and 18 O.

Elements	Average	Minimum	Maximum
SiO_2 (wt.%)	66.99	65.87	67.89
Al_2O_3	16.96	16.64	17.38
TiO_2	0.02	0.00	0.07
FeOtot.	0.82	0.50	1.36
Cr_2O_3	0.02	0.00	0.13
MgO	0.01	0.00	0.03
MnO	0.02	0.00	0.09
CaO	0.01	0.00	0.03
Na_2O	0.18	0.00	0.45
K_2O	0.01	0.00	0.04
Cs_2O	0.01	0.00	0.03
BeO*	13.72	13.55	13.90
H_2O**	1.07	0.00	1.75
Total	98.74	97.51	99.94
Si (apfu)	6.09	6.06	6.13
Al	1.82	1.79	1.88
Ti	0.00	0.00	0.01
Fe	0.06	0.04	0.10
Cr	0.00	0.00	0.01
Mg	0.00	0.00	0.00
Mn	0.00	0.00	0.01
Ca	0.00	0.00	0.00
Na	0.03	0.00	0.08
K	0.00	0.00	0.01
Cs	0.00	0.00	0.01
Be*	3.00	3.00	3.00

The meaning of the symbols: * = stoichiometric calculations, ** = stoichiometric calculated using the equation $H_2O = (0.5401 \times lnNa_2O) + 2.1867$ (Marshall *et al.*, 2016), and *** = ideal value for stoichiometric calculations.

The microanalyses were performed on a section perpendicular to the c-axis of the aquamarine crystal, following concentric growth zones (from edge to core) through profiles with spots approximately equidistant to each other (some of the analyses are shown in the Figures 2c and 2d). EPMA results revealed that the most important chromophore element for aquamarine is the FeO_{total} (Fe^{3+} and Fe^{2+}), followed by some content trace of TiO_2, MnO and Cr_2O_3 (Fig. 2d), which are close or below to the detection limit. Furthermore, it is important to note the irregular and low Na content, as well as the very low K, Ca and Mg contents (between 0 - 0.04 wt.%). A tendency for positive correlation between Fe+Mg and Na is observed (Fig. 2d and 2e), indicating the importance role of these compensating alkali ions. However, it is possible to note important variations on the Fe and Na contents: remarkable loss of Na at the edges, followed by progressive enrichment in the intermediate zone and ending with decreasing of Fe and Na in the central part of the aquamarine crystal. On the other hand, there is a tendency for negative cationic correlation between Al and the sum of Fe + (Mg, Ti, Cr, Mn), which indicates that the major replacement process of these elements takes place within Al-octahedra site (Fig. 2f). The other trace elements with chromophore function (*i.e.*, Ti, Cr, Mn) have negligible participation (content below 0.10 wt.%), but it is probable that some content of these trace elements also was accommodated to the Be-tetrahedra site (*e.g.*, Aurisicchio *et al.*, 1988; Hawthorne and Huminicki, 2002).

5. Fluid inclusion data

The petrographic study, at room temperature (±25° C), identified only aqueous primary and secondary/pseudo-secondary fluid inclusions. The primary fluid inclusions occur isolated or in small groups, frequently followed the concentric growth zone, with size between 10-75 μm, composed of mono- and biphasic morphology. On the other hand, the aquamarine crystals exhibit some microfractures or deformation features that contain fluid inclusions less than 10 μm in size and

showed monophasic morphology. These fluid inclusion types were classified as secondary or pseudo-secondary. This study addresses only the primary fluid inclusions, which display adequate sizes for microthermometric observations.
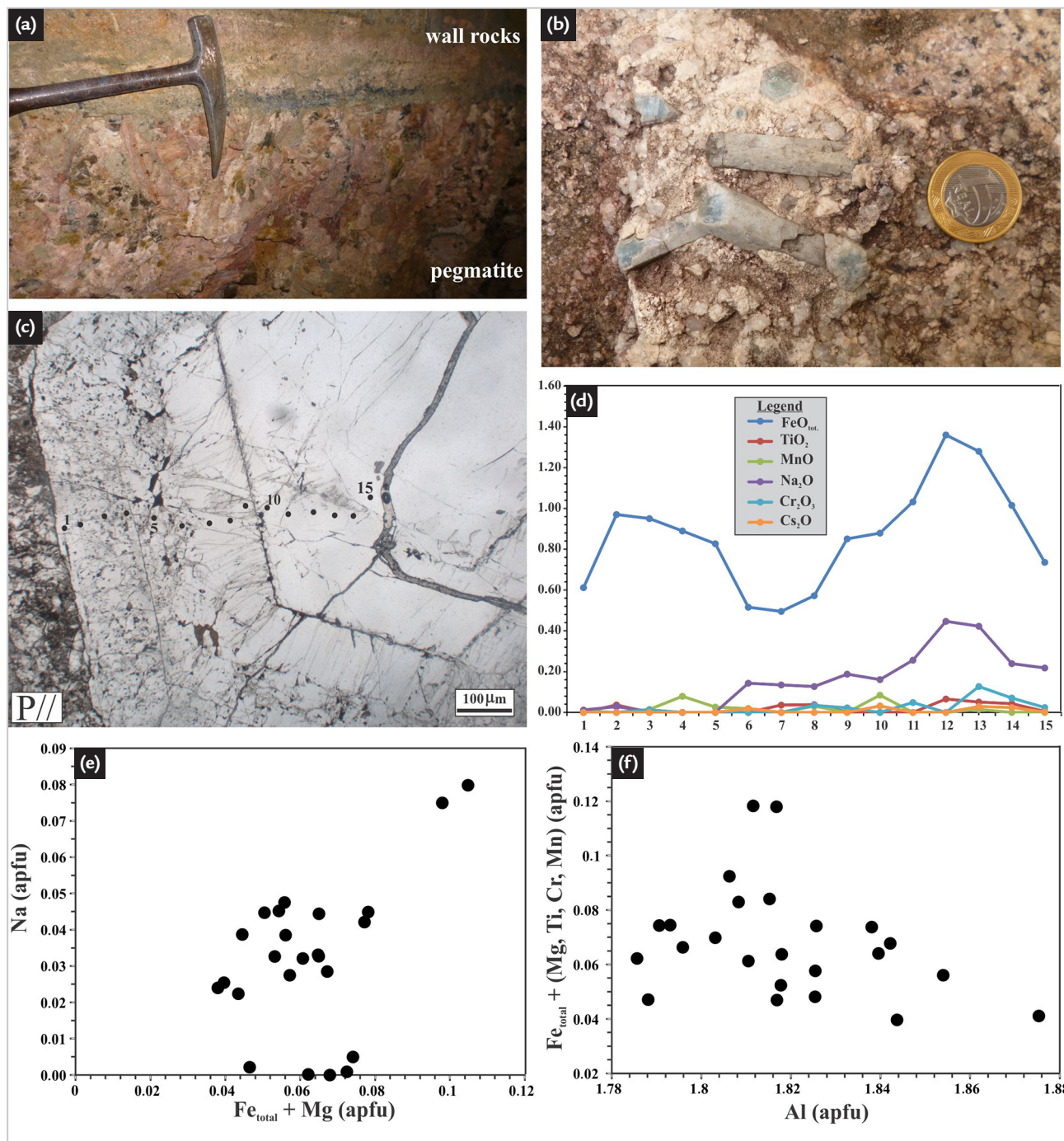

Figure 2 - a) Contact zone between tabular zoned pegmatite body and Jamari Complex wall-rocks; b) Euhedral short to long aquamarine crystals within granitic pegmatite, showing concentric growth zones and irregular coloration; c) photomicrography of a concentrically zoned aquamarine crystal. Note several micro-inclusions distributed mainly along the growth lines, as well as a set of electron-microprobe analyses along a crystal profile from edge to core (P// = parallel polars); d) Weight percent data for some selected oxides in aquamarine along a traverse. Note the tendency for positive correlation between Fe_2O_{3total} and Na_2O; e) Cationic correlation between Fetotal + Mg *vs* Na (in *apfu*); and F) Cationic correlation between Al^{3+} *vs* sum of Fe_{total} + (Mg, Ti, Cr, Mn) (in *apfu*).

5.1 Petrography

Two morphological types of primary aqueous fluid inclusions were identified and divided into: type 1 and type 2:

• Type 1 is most common and shows sizes between 40-75 μm. It is composed of two immiscible phases: liquid-rich inclusions with a vapor bubble (liquid + vapor). The liquid phase shows colorless to slightly gray color and low birefringence, while the vapor phase exhibits dark gray to black color. The vapor/liquid volumetric ratios (F factor) vary from 10 to 25%. However, morphological variations lead to subdivision of type 1 into: 1a and type 1b. The type 1a shows sub-rounded to irregular shapes with F = 10-20% (Fig. 3a). Occasionally, type 1a occurs hosting a solid phase, characterized by sub-rounded opaque micro-crystals with a size smaller than 5 μm (Fig. 3b).

On the other hand, the type 1b presents elongated to cylindrical shape with F = 20-25%, usually parallel to the c-axis (Fig. 3c).

• Type 2 are monophasic, composed by a liquid phase. It shows a sub-rounded to elliptical shape, colorless to slightly gray color, low birefringence and size below 10 μm (Fig. 3d).
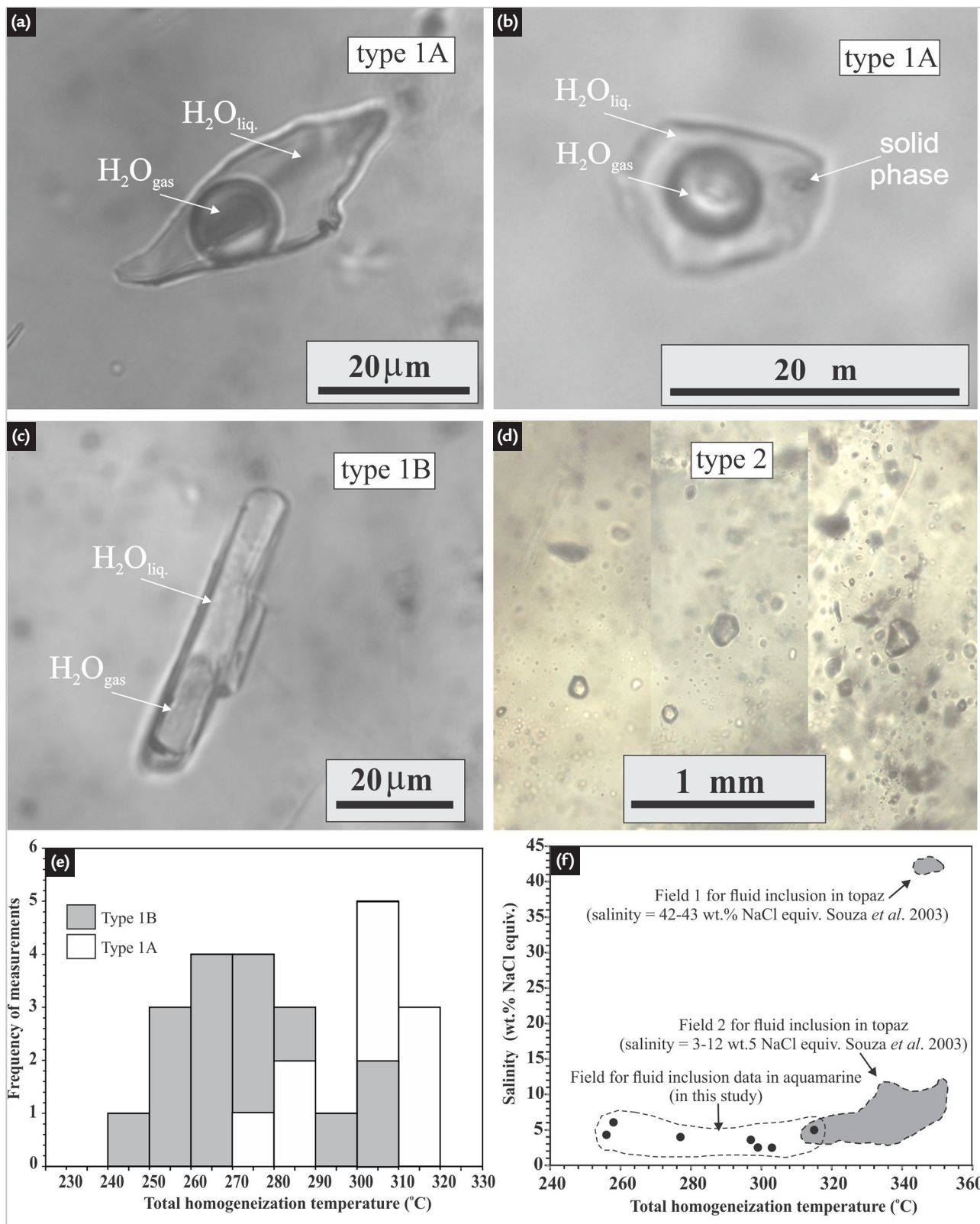

Figure 3 - Morphological features of main aqueous fluid inclusion types identified in the aquamarine crystals. a) and b) Morphological variation from type 1a aqueous fluid inclusions. Note in b, the type 1a sub-rounded shape and hosting an opaque micro-crystal (solid phase); c) Type 1B with cylindrical shape often found parallel to the c-axis; d) Type 3 fluid inclusion with sub-rounded to elliptical shape; e) Frequency histogram of total homogeneization temperatures (Thtot) of aqueous fluid inclusions at aquamarine (types 1a and 1b); and f) Total homogeneization temperatures vs salinity diagram applied to fluid inclusions data obtained in aquamarine. For a simple comparative analysis on the fluid inclusion data in gems from Massangana pegmatites available in literature. We have also included in this diagram the fluid inclusion data obtained from topaz and reported by Souza *et al.* (2003).

5.2 Microthermometry

Approximately 20 fluid inclusions were analyzed. During the to-freezing stage (below -100° C), it was observed that the vapor + liquid phases make up an aqueous fluid system ($H_2O_{(vapor)}$ + $H_2O_{(liquid)}$). In this context, only a few type 1 and type 2 fluid inclusions showed appropriate size for observing the change phase for eutectic and ice final melt temperatures. The eutectic temperature was estimated between -22.2° and -20.1° C, while the ice final melt (Tm ice) varied from -2.2° to -1.1° C (Tab. 2). These data point for a H_2O-NaCl fluid system (*e.g.*, Shepherd *et al.*, 1985; Bodnar and Vityk, 1994). The salinity was estimated from Tm ice, which varies from 6 to 2.5 wt.% NaCl equivalent, after applied the equation proposed by Bodnar (1993).

Table 2 - Microthermometric data summary on fluid inclusions obtained in aquamarine.

Fluid inclusion types	Microthermometric Intervals			
	T eut. (°C)	Tm. Ice (°C)	Th total (°C)	Salinity (% wt. NaCl equiv.)
Type 1A	-22.2 to -20.1	-2.2 to -1.1	258.4 – 210.4	2.5 to 6.0
Type 1B			243.2 – 314.8	
Type 2	-21.4 to -20.4		–	

During the heating stage, the contraction of the vapor phase occurred until blending into the liquid phase (L + V → L) at the total homogeneization temperatures (Thtot.) between 243°-315° C (Fig. 3e). On the other hand, the final melt temperatures of solid phase from type 1B fluid inclusion were not measured, due to crepitation of some fluid inclusions at temperatures close to 400° C. Probably this solid phase corresponds to minerals captured together with liquid-gas mixtures from hydrothermal solutions during formation of cavities. The fluid density was estimated around 0.95 g/cm³, on base Thtot. vs salinity correlation (Shepherd *et al.*, 1985).

6. Discussion

The color changes in beryl crystals are directly connected to the entrance in the crystalline structure of chromophore elements in the Al-octahedra site (Hawthorne and Huminicki, 2002). However, the geological setting has an important role in this chemical-replacement mechanism, which can be linked to fractional crystallization and metasomatism processes, for example (*e.g.*, Simmons and Webber, 2008; Groat *et al.*, 2008). The beryl-aquamarine variety linked to fractional crystallization of granitic-pegmatite phase is a result of nucleation and growth of crystals controlled by temperature decrease. In association, the entrance of Fe within the Al-bearing site is the main mechanism responsible for the blue color (Beal and Lentz, 2002; Viana *et al.*, 2002, Groat *et al.*, 2010).

Aquamarine from Massangana batholith has the Fe as the main cromophore element. The negative correlation between Al *vs* Fe ± (Mg, Ti, Cr, Mn) associated to positive correlation between Fe + Mg *vs* Na, indicates that the major cationic replacement mechanism occurred within the octahedral Al-site. On the other hand, alkali ions (mainly Na, followed by some K and Ca content) and H_2O enter in the channel sites, positioning between the six-membered rings of Si tetrahedral of beryl structure, thus maintaining the charge balance (Sampaio Filho *et al.*, 1973; Aurisicchio *et al.*, 1988; Sherriff *et al.*, 1991; Groat *et al.*, 2002).

The growth of aquamarine from Massangana batholith is marked by internal variations in color and chemical composition. The reasons for these variations are unclear. However, it is probable that some type of geochemical imbalance within the environment of growth leads mainly to lack of or irregular supply of Fe and Na. This imbalance then favored color (from light blue to blue) and chemistry oscillation, respectively. According to Aurisicchio *et al.*, (1988), zoning can occur because of chemical restrictions of the environment (bulk-rock chemistry and fluid-phase composition) or exchange reactions with other minerals, which can be influenced by changes in pressure, temperature and pH parameters. On the other hand, based on x-ray diffraction, Mössbauer, infrared and UV-visible spectra data, previous studies have shown that color change in beryl may be linked to charge imbalance created during the growth, relative to the proportion of Fe^{3+} in the octahedral sites and of Fe^{2+} in the channel sites (Viana *et al.*, 2002; Groat *et al.*, 2010).

H_2O-rich fluid phases are common in fractionated granitic melts emplaced at the upper crust (Bodnar, 1995; Roedder and Bodnar, 1997). Thermometry data indicate that the final temperatures in pegmatite pocket zones range from 390° to 240° C (London, 1992; Johnson *et al.*, 2002). Previous studies on the fluid inclusion in topaz, reported by Souza *et al.* (2003), associated with fluid inclusion data of aquamarine presented in this study, corroborated with the essentially aqueous (H_2O-NaCl) nature of the paleofluids in the Massangana pegmatites. However, important microthermometric differences between theses paleofluids can be observed. For example: paleofluids from topaz show different intervals of salinity (3-12 and 42-43 wt.% NaCl equiv.), density (0.65- 0.75 and above 1.2 g/cm³) and Thtotal between 320°-350° C, indicating a fluid mixing process during evolution and cooling (Souza *et al.*, 2003). On the other hand, paleofluids from the aquamarine show low salinity (2.5 - 6 wt.% NaCl equiv.), density around 0.95 g/cm⁻³ and Thtotal between 315°-243° C. These microthermometric data indicate that for topaz, this is linked to the fluids with variable salinity and higher temperatures, while for aquamarine, it is tied to fluids with lower salinity and temperature (Fig. 3f). Therefore, it is likely that the temperature decrease associated with the pressure drop and decrease in salinity

in pegmatites pocket zone (*e.g.*, London, 2008), accompanied by mixing with others aqueous fluids from the upper crust (*e.g.*, Hedenquist 1995), were important mechanisms in the crystallization history of the Massangana pegmatites.

7. Concluding remarks

The data presented in this study led us to the following conclusions:

• The aquamarine is linked to the fractional crystallization in the granitic-pegmatites phase. It is the result of nucleation and growth of crystals in the pocket zone, controlled by temperature decrease and marked by a concentric zoning and irregular color;

• The microthermometry data indicate that the aquamarine growth under an aqueous (H_2O-NaCl) fluid system with low salinity, low density e total homogenization temperature between 243°-315° C, is compatible to final temperatures in pegmatites pocket zone.

• Fe is the main chromophore element, which replaces the octahedral Al-site. This can be demonstrated by a negative correlation between Al and Fetotal.

On the other hand, the alkalis (mainly Na), occupy the channel sites together with H_2O, and have an important role in the charge balance;

• The internal variations in color and chemical composition in aquamarine are mainly attributed to some type of geochemical imbalance that led to the lack or irregular supply of Fe and Na within the environment of growth.

References

ARTIOLI, G.; RINALDI, R.; STAHL, K.; ZANAZZI, P. F. Structure refinements of beryl by single-crystal neutron and X-ray diffraction. *American Mineralogists,* v. 78, p. 762-768, 1993.

AURISICCHIO, C.; FIORAVANTI, O.; GRUBESSI, O.; ZANAZZI, P. F. Reappraisal of the crystal chemistry of beryl. *American Mineralogists,* v. 73, n. 7-8, p. 826-837, 1988.

BARRETO, S. B.; BITTAR, S. M. B. The gemstone deposits of Brazil: occurrences, production and economic impact. *Boletín de la Sociedad Geológica Mexicana,* v. 62, n. 1, p.123-140, 2010.

BEAL, K-L.; LENTZ, D. R. Aquamarine beryl from Zealand Station, Canada: a mineralogical and stable isotope study. *Journal of Geosciences,* v. 55, n. 1, p. 57-67, 2002. DOI: http://dx.doi.org/10.3190/jgeosci.059.

BETTENCOURT, J. S.; TOSDAL, R. M.; LEITE Jr., W. B.; PAYOLLA, B. L. Mesoproterozoic rapakivi granites of the Rondônia Tin Province, southwestern border of the Amazonian craton, Brazil – I. Reconnaissance U-Pb geochronology and regional implications. *Precambrian Research,* v. 95, n. 1-2, p. 41-67, 1999.

BODNAR, R. J. Revised equation and table determining the freezing point depression of H2O-NaCl solutions. Geochimica et Cosmochimica Acta, v. 57, p. 683-684, 1993. DOI: 10.1016/0016-7037(93)90378-A.

BODNAR, R. J.; VITYK, M. O. Interpretation of microthermometric data for H_2O-NaCl fluid inclusions. *In*: DE VIVO, B.; FREZZOTTI, M. L. (ed.). *Fluid inclusions in minerals:* methods and applications: short course of the working group (IMA) "Inclusions in Minerals", Pontignano-Siena, 1994. Blacksburg, VA: Virginia Tech, 1994. p. 117-130.

BODNAR, R. J. Fluid inclusion evidence for a magmatic source for metals in porphyry copper deposits. In: THOMPSON, J. F. H. (ed.). *Magmas, fluids and ore deposits.* Canada: Mineralogical Association of Canada, 1995. p. 39-152. (Short course series, v.23).

DEBOWSKI, B. P.; REIS, M. J.; VIANA, R. R. Caracterização química e mineralógica de topázios do Complexo Massangana, região central de Rondônia. *In:* SIMPÓSIO DE GEOLOGIA DO CENTRO-OESTE, 13., 2013, Cuiabá. *Anais [...].* Cuiabá: SGCO, 2013.

DEBOWSKI, B. P. *Caracterização petrológica de Maciços das Suítes Intrusivas Rondônia e Serra da Providência com base em dados litogeoquímicos e petrográficos e isotópicos (U-Pb e Lu-Hf) em zircão.* 2016. 117 f. Dissertação (Mestrado em Geociências) – Faculdade de Geologia, Universidade do Estado do Rio de Janeiro, Rio de Janeiro, 2016.

GROAT, L. A.; MARSHALL, D. D.; GIULIANI, G.; MURPHY, D. C.; PIERCEY, S. J.; JAMBOR, J. L.; MORTENSEN, J. K.; ERCIT, T. S.; GAULT, R. A.; MATTEY, D. P.; SCHWARZ, D.; MALUSKI, H; WISE, M. A.; WENGZYNOWSKI, W.; EATON, D. W. Mineralogical and geochemical study of the Regal Ridge Emerald Showing, Southeastern Ukon. *The Canadian Mineralogist,* v. 40, n. 5, p. 1313-1338, 2002.

GROAT, L. A.; GIULIANI, G.; MARSHALL, D. D.; TURNER, D. Emerald deposits and occurrences: a review. *Ore Geology Reviews,* v. 34, n. 1-2, p. 87-112, 2008. DOI: https://doi.org/10.1016/j.oregeorev.2007.09.003.

GROAT, L. A.; ROSSMAN, G. R.; DYAR, M. D.; TURNER, D.; PICCOLI, P. M. B.; SCHULTZ, A. J.; OTTOLINI, L. Crystal chemistry of dark blue aquamarine from the true blue showing, Ukon Territory,

Canada. *The Canadian Mineralogist,* v. 48, n. 3, p. 597-613, 2010. DOI:10.3749/canmin.48.3.597.

HAWTHORNE, F. C.; HUMINICKI, D. M. C. The crystal chemistry of beryllium. In: GREW, E. S. (ed.). *Beryllium:* mineralogy, petrology and geochemistry. [*S. l.*]: [*s. n.*], 2002. p. 333–403. (Reviews in Mineralogy & Geochemistry, v. 50).

HEDENQUIST, J. W. The ascent of magmatic fluid: discharge versus mineralization. *In:* THOMPSON, J. F. H. (ed.). *Magmas, fluids and ore deposits.* Canada: Mineralogical Association of Canada, 1995. p. 263-289. (Short course series, v.23).

ISOTTA, C. A. L.; CARNEIRO, J. M.; KATO, H. T.; BARROS, R. J. L. *Projeto Província Estanífera de Rondônia:* relatório final. Porto Velho: MME/DNPM/CPRM, 1978. 407p.

JOHNSON, S.E., SCHIMIDT, K.L., TATE, M.C. Ring complexes in the Peninsular Tanges Batholith, Mexico and the USA: magma plumbing systems in the middle and upper crust. *Lithos,* v.61, p.187-208, 2002.

KLOOSTERMAN, J. B. Ring-structures in the Oriente e Massangana granite complexes, Rondônia, Brasil. *Revista de Engenharia, Mineração e Metalurgia,* v. 45, n. 266, p. 73-77, 1967.

KLOOSTERMAN, J. B. Uma província do tipo nigeriano no sul da Amazônia (Parte 1). *Revista de Engenharia, Mineração e Metalurgia,* v. 47, n. 278, p. 59-64, 1968.

LEAL, J. W. L.; SILVA, G. H.; SANTOS, D. B.; TEIXEIRA, W.; LIMA, M. I. C.; FERNANDES, C. A. C.; PINTO, A. C. Geologia. *In*: PROJETO RADAMBRASIL. *Folha SC.20 Porto Velho:* geologia, geomorfologia, pedologia, vegetação, uso potencial da terra. Rio de Janeiro: DNPM, 1978. p. 19-184. (Levantamento de Recursos Naturais, v. 16).

LONDON, D. The application of experimental petrology to the genesis and crystallization of granitic pegmatites. *The Canadian Mineralogist,* v. 30, n. 3, p. 499-540, 1992.

LONDON, D. *Pegmatites.* [*S. l.*]: The Mineralogical Association, 2008. 347p. (The Canadian Mineralogist, Special Publication n.10).

MARSHALL, D.; DOWNES, P. J.; ELLIS, S.; GREENE, R.; LOUGHREY, L.; JONES, P. Pressure–temperature–fluid constraints for the Poona emerald deposits, Western Australia: fluid inclusion and stable isotope studies. *Minerals,* v. 6, n. 4, p. 130, 2016.

MOROSIN, B. Structure and thermal expansion of beryl. *Acta Crystallographica,* v. 28, p. 1899-1903, 1972. DOI: https://doi.org/10.1107/S0567740872005199.

OKIDA, R. *Aplicação do sensoriamento remoto e aerogamaespectrometria ao estudo do controle estrutural dos granitos estaníferos de Rondônia.* 2001. 217 f. Tese (Doutorado em Geociências) - Instituto de Geociências, Universidade de São Paulo, São Paulo, 2001.

PRIEM, H. N. A.; BOELRIJK, N. A. I. M.; HEBEDA, E. H.; VERSCHURE, R. H.; BOM, E. H. Isotopic age of tin granites in Rondônia, N.W. Brazil. *Geologie en Mijnbouw,* v. 45, p. 191-192, 1966.

PRIEM, H. N. A.; BOELRIJK, N. A. I. M.; HEBEDA, E. H.; VERDURMEN, E. A. TH.; VERSCHURE, R. H.; BOM, E. H. Granitic complexes and associated tin mineralizations of "Grenville" age in Rondônia, western Brazil. *Geological Society of America Bulletin,* v. 82, n. 4, p. 1095-1102, 1971.

ROEDDER, E.; BODNAR, R. J. Fluid inclusions studies of hydrothermal ore deposits. *In:* BARNES H. L. (ed.). *Geochemistry of Hydrothermal Ore Deposits.* 3ª ed. New York: John Wiley CO., 1997. p.657-697.

ROMANINI, S. J. *Geologia e geoquímica do complexo granitóide de Massangana e sua relação com as mineralizações de estanho.* 1982. 85 f. Dissertação (Mestrado em Geologia) – Instituto de Geociências, Universidade Federal da Bahia, Salvador, 1982.

SAMPAIO FILHO, H. A.; SIGHNOLFI, G. P.; GALLI, E. Contribution to the crystal chemistry of beryl. *Contribution to Mineralogy and Petrology,* v. 38, p. 279-290, 1973.

SERVIÇO GEOLÓGICO DO BRASIL. *Geologia e recursos minerais do estado de Rondônia:* Sistema de Informações Geográficas - SIG: texto explicativo do mapa geológico e de recursos minerais do estado de Rondônia – Escala 1:1.000.000. Porto Velho: CPRM, 2007. 153p. 1 CD-ROM.

SHEPHERD, T. J.; RANKIN, A. H.; ALDERTON, D. H. M. *A practical guide to fluid inclusion studies.* New York: Chapman and Hall, 1985. 239 p.

SHERRIFF, B. L.; GRUNDY, H. D.; HARTMAN, J. S.; HAWTHORNE, F. C.; CERNY, P. The incorporation of alkalis in beryl: multi-nuclear MAS NMR and crystal-structure study. *Canadian Minerologist,* v. 29, p. 271-285, 1991.

SIMMONS, W. B.; WEBBER, K. Pegmatite genesis: State of the art. European Journal of Mineralogy, v. 20, n. 4, p. 421-438. 2008. DOI: 10.1127/0935-1221/2008/0020-1833.

SOUZA, V. S.; PONTES, R. M.; MOURA, M. A. Inclusões fluidas em topázio do Complexo Granítico Estanífero de Massangana (RO). *REM - Revista Escola de Minas,* v. 56, n. 4, p. 231-236, 2003.

VIANA, R. R.; JORDT-EVANGELISTA, H.; COSTA, G. M.; STERN, W. B. Characterization of beryl (aquamarine variety) from pegmatites of Minas Gerais, Brazil. *Physics and Chemistry of Minerals,* v. 29, n. 10, p. 668–679, 2002. DOI: 10.1007/s00269-002-0278-y.